sciendo

Investigation into Increasing the Motor-Drivable Current Using a Thermoelectric Cooling Module

Research paper

Kazuma Morikawa, Seiichiro Katsura*

Department of System Design Engineering, Keio University, Yokohama, Japan

Abstract: To enhance the performance of humanoids, mobile robots and manipulators, motors are desired to be able to provide high torque without relying on gears. To be able to drive joint motors with high output, the current value that can flow needs to be increased. However, the heat generated by the high current drive can cause motor failure, so cooling is necessary. We used thermoelectric cooling as a new cooling method for high-power drive of motors. By developing a thermoelectric cooling module for motors and conducting experiments, the effectiveness of thermoelectric cooling was verified. In the experiment, the motor was kept running at a high current for a long period of time. The comparison with the motor alone or with water cooling showed that the thermoelectric cooling module can significantly reduce the rise in temperature of the motor. Furthermore, based on the results of the voltage value measurements, it was expected that the increase in coil resistance due to higher coil temperatures would be kept lower than in other cases. The effect on rise in internal temperature was also considered to be greater than that of water cooling. These experimental results show that the thermoelectric cooling module can be used to increase the upper limit of the current at which the motor is continuously driven.

Keywords: motor • cooling • thermoelectric effect • Peltier devices • high power

1. Introduction

To enhance the performance of humanoids, mobile robots and manipulators, motors are desired to be able to provide high torque (Guizzo, 2019; Seok et al., 2015). They must be able to withstand sudden external forces and temporarily high loads in contact with the outside world. On the other hand, just maintaining the body posture requires a large amount of force at the joints. In addition to high power drive during a moment, it needs to be able to achieve continuous high-power drive.

However, because electromagnetic motors alone do not provide enough torque, gears are used, and gear ratios tend to be large. Although gears can increase torque, there is a trade-off between speed and torque, resulting in slower movement. Large gear ratios are also problematic from the standpoint of back-drivability. When operating in the same environment as humans, low back-drivability is dangerous because it makes the robot stiff when it comes into contact with humans. A low gear ratio is also better for delicate control such as force control, so that the robot can respond softly to external forces like a human or an animal (Katsura et al., 2003, 2008). In recent years, cooperative robots have been used a lot, but mainly in specific areas, such as factories, where access by the general public is restricted. The ability of the joints to respond softly to unexpected contact allows for closer contact with a variety of people and safer dynamic movement around people. Therefore, it is essential to increase the power of the motor itself.

In order to enable large power output with respect to the motor alone, rather than increasing torque through gears or other mechanisms, many studies have been conducted to improve the internal magnetic field so that the output relative to the current is increased. They include the use of Halbach arrays of magnets (Kumar and Kumar, 2016;

* Email: katsura@sd.keio.ac.jp

Liu et al., 2018) and new magnetic materials (Nizam et al., 2014; Ramesh and Lenin, 2019). On the other hand, when high current is applied for high-power operation, a lot of heat is generated from the windings.

In robots, heat affects performance because electronic components and devices have ideal working temperatures, and excessive increases in temperature can cause failures. Management of heat is important, and forced cooling, heat-dissipating components and materials that enhance heat conduction are being researched and utilised (Sevinchan et al., 2018). In robot joint motors, thermal burnout of windings and demagnetisation of permanent magnets are also major causes of motor damage. It is necessary to limit the current flow so that the temperature does not exceed a certain level (Kumagai et al., 2014; Kawaharazuka et al., 2020). By facilitating heat dissipation and reducing heat generation, motors are able to carry a large current.

To enable high-output drive, motors with a built-in fan that rotates with the motor shaft are commercially available. In addition to air cooling, research is also being conducted to increase motor power by using liquids for forced cooling. The use of liquid cooling increases the cooling performance of motors compared to air cooling and increases the range of current flow, which in turn increases the speed and torque. Urata et al. (2010) developed a high-speed, high-torque module for humanoids using liquid cooling for the motor. Kim et al. (2018) also developed a leg actuator that incorporates cooling using a viscoelastic liquid. On the other hand, our research uses the thermoelectric effect as a new cooling method for high current flow to the motor of a joint. Then, we evaluate the method.

The following studies have been conducted on the use of thermoelectric effect in motors. Toren and Mollahasanoglu (2021) fabricated a heat dissipation system that combines an induction motor with a Peltier device and a fan, and they showed that the motor temperature was maintained lower than that using the fan alone. Siyang et al. (2016) developed a motor exhaust heat power generation system that converts thermal energy from the motor exhaust heat into electrical energy through the Seebeck effect and then evaluated its performance.

We have developed a thermoelectric cooling module to apply thermoelectric cooling to motors. One of the major features of thermoelectric cooling modules is that the motor temperature can be significantly lowered in advance. This is effective for very-short-time drives. On the other hand, this study examines the effects of continuous current flow over an extended period of time without prior cooling.

In addition, while many studies have been conducted to investigate changes in motor performance by changing the structure of the motor itself (Gwoździewicz and Zawilak, 2016; Quintal-Palomo et al., 2016; Sarac and Stefanov, 2020), this research does not make any changes to the motor itself and uses the cooling method that can be applied to various motors. In particular, the DC motors used in the experiments in the paper are not suitable for cooling because the coils, the main source of heat, are located inside the motor and have high thermal resistance. We show that the proposed method is effective even in such cases.

2. Thermoelectric Cooling Module for Motors

2.1. Appearance and usage of the thermoelectric cooling module
We have developed a thermoelectric cooling module as shown in Figure 1. A motor is fixed inside, and the motor can be cooled by driving Peltier devices. When the Peltier devices are driven, a tube is connected to the outer fitting to circulate water inside the module.

2.2. Peltier device
Peltier devices used in the thermoelectric cooling module are described. Figure 2 shows an image of the Peltier device used, with a note on the heat transfer. A Peltier device is a semiconductor device capable of transferring heat using the thermoelectric effect, consisting of n-type and p-type semiconductors alternately joined by metal, which generates the Peltier effect, a type of thermoelectric effect, when a current flows (Pourkiaei et al., 2019). It can be driven simply by connecting a DC current and is used for small refrigerators. It can perform cooling, heating and temperature control by controlling the electric current; moreover, it has the advantages of good temperature response and low noise. It is also used for thermoelectric power generation that generates electrical energy from temperature differences (Alencar Almeida et al., 2015; Belovski et al., 2021).
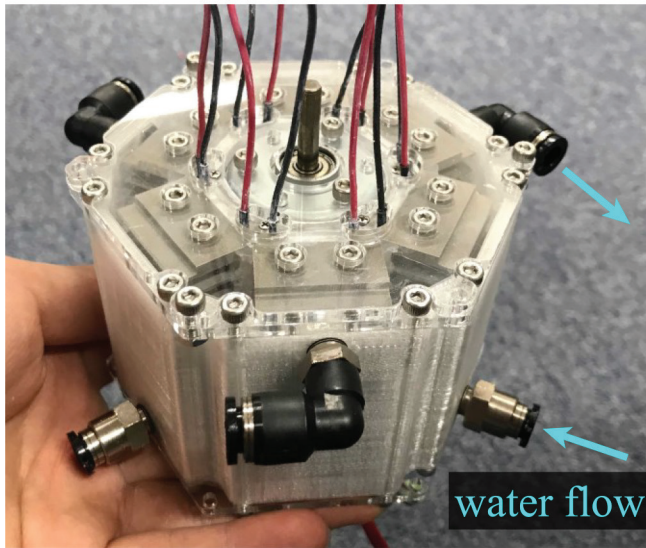
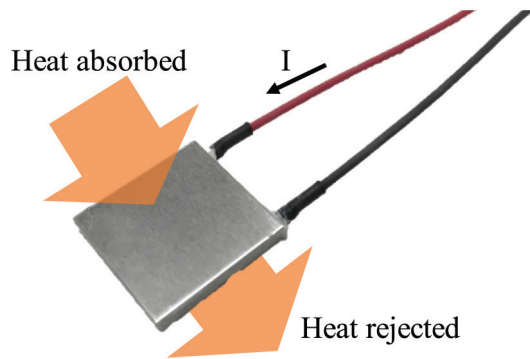**Fig. 1.** Photograph of the thermoelectric cooling module.

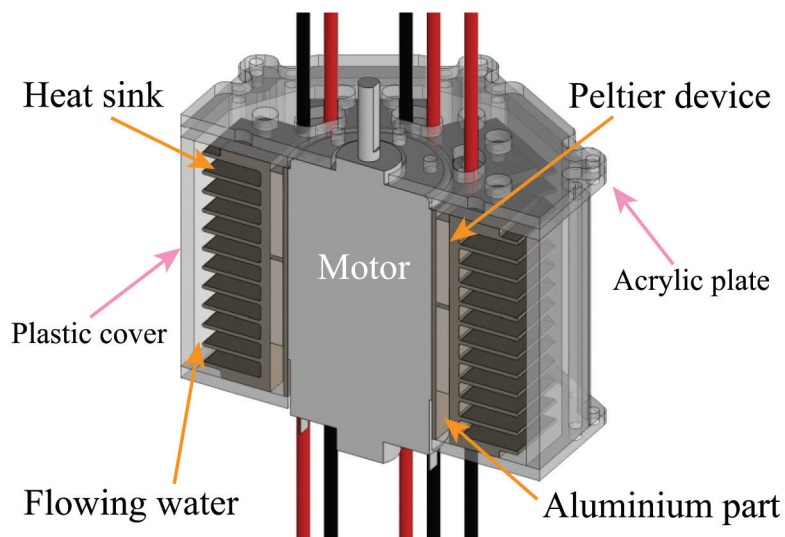**Fig. 2.** Heat transfer by the Peltier device.

Fig. 3. Schematic diagram of the cross-sectional view of the thermoelectric cooling module (fittings for water flow are omitted).

2.3. Structure of the thermoelectric cooling module

The internal structure is described below. A cross-sectional view of the thermoelectric cooling module is shown in Figure 3. An aluminium part in the shape of a cylinder hollowed out from a hexagonal cylinder is in contact with the motor, and 12 Peltier devices are present on its surface. A heat sink is in contact with the outside of the Peltier devices. To facilitate heat transfer, each contact area is coated with silicon for heat dissipation. Water flows between the heat sink and the outermost plastic cover. The water is pushed out by a pump and flows through a tube connected to the plastic cover, through the thermoelectric cooling module and cools the heat sink. If the heat dissipation surface of the Peltier devices is inadequate, sufficient cooling effect cannot be obtained, so heat sinks and water cooling are used.

3. Experimental Equipment and Methods

3.1. Equipment

The experimental setup is shown in Figure 4. A DC motor (DMN37HB; Nidec-Servo, Gunma, Japan) is used as the motor to be measured. The DC motor is connected to a stabilised power supply (PAS160-6; Kikusui, Yokohama, Japan). The DC motor is connected to the load motor (SGMCS-02BDC41; Yaskawa, Fukuoka, Japan) via a coupling. The load motor is used only as a load and is not driven.

A temperature sensor called a thermistor (103JT-050; Semitec, Tokyo, Japan) is used to measure the temperature. The temperature sensor is fixed such that it is in contact with the bottom of the motor, as shown in Figure 4. In addition, the approximate change in voltage values output from the stabilised power supply is recorded.

In Figure 4, the DC motor is fixed to the thermoelectric cooling module, but to make a comparison, the thermoelectric cooling module (A) is replaced and experiments are also conducted with water cooling (B) and a single motor (C). The three patterns to be experimented are shown below:

(A)   Thermoelectric cooling module
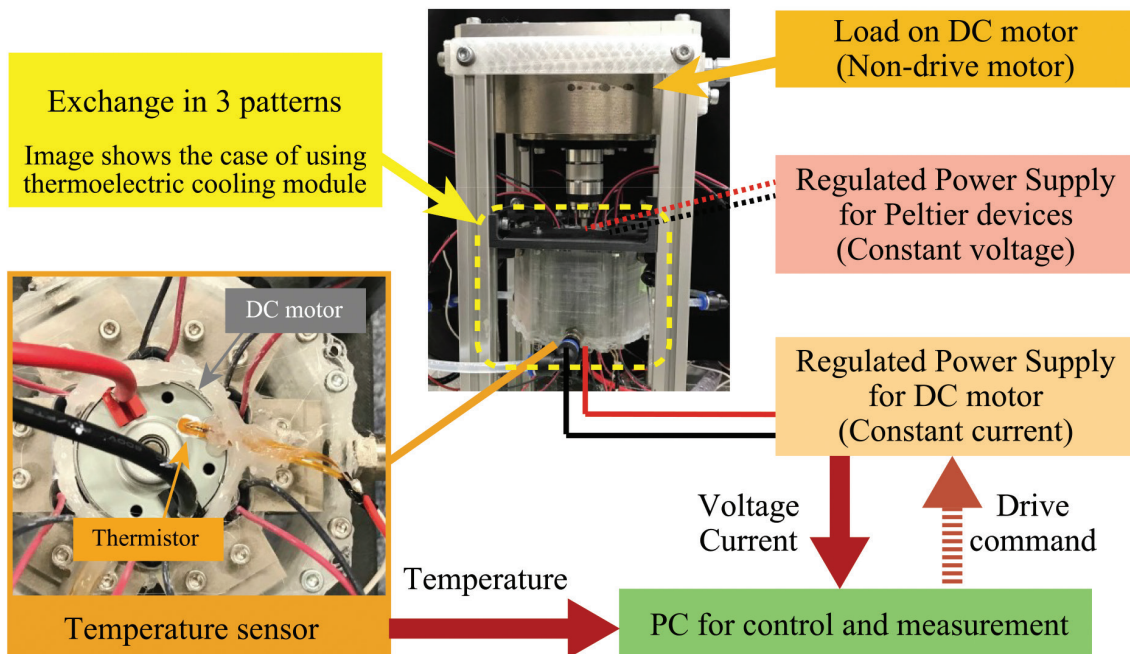(B)   Water cooling: flowing water and heat sinks
(C)   No cooling: motor alone

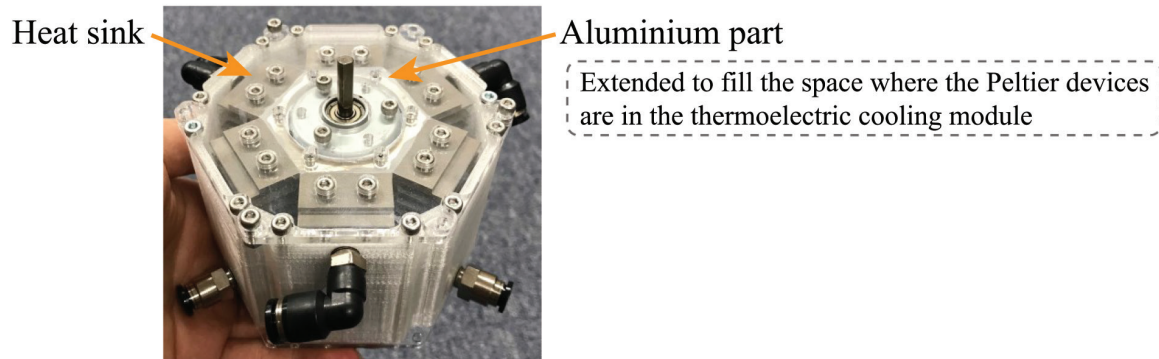**Fig. 4.** Diagram of the experimental equipment.

Heat sink — Aluminium part

Extended to fill the space where the Peltier devices are in the thermoelectric cooling module

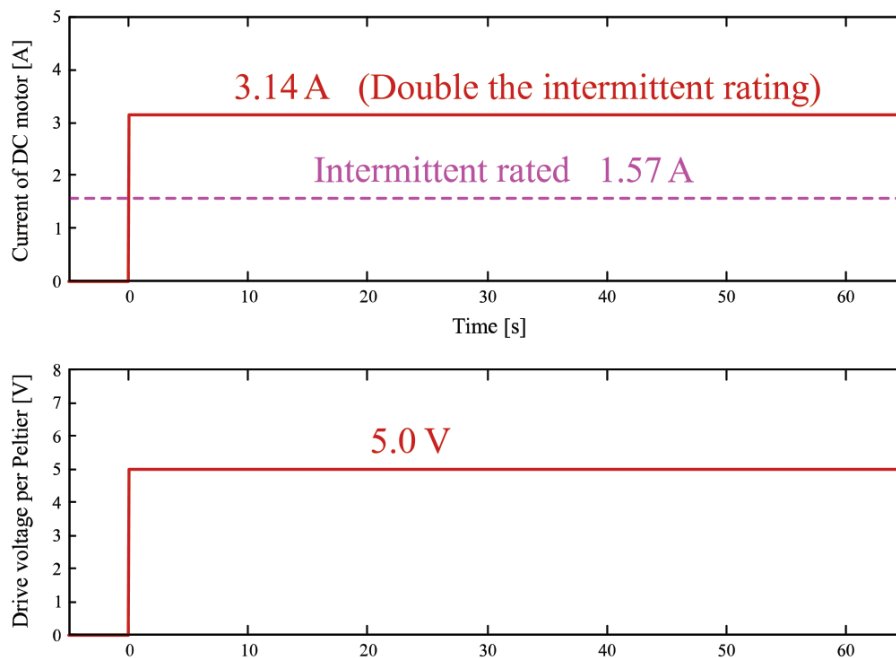**Fig. 5.** Photograph of the water-cooling mechanism.

Fig. 6. Command values for driving DC motors and Peltier devices.

The structure of the water-cooling mechanism, made for comparison, is shown in Figure 5. The structure of the water-cooling mechanism is such that the Peltier devices are removed from the thermoelectric cooling module, and the aluminium parts in contact with the motor are enlarged to fill the space where the Peltier devices used to be. The structure of the heat sink and water cooling is the same as that of the thermoelectric cooling module.

3.2. Method

We measure the temperature of the DC motor's surface (bottom surface) when the DC motor is driven at a constant current. In addition, the voltage values applied to the DC motor are also recorded. In the case of thermoelectric cooling modules, the drive of the Peltier devices is started at the same time as the DC motor starts driving. Water circulation in case of thermoelectric cooling module and water cooling is done before the DC motor drive.

The motor current command value is 3.14 A, as shown in Figure 6. This value is twice the value of the intermittent rating. Note that in this experiment, the motor is driven in continuous operation, not intermittent operation. As reference data, temperatures were also measured for continuous operation at 1.57 A without cooling.

The thermoelectric cooling module uses 12 Peltier devices, and a constant voltage of 5 V on average (15 V in series of three) is applied to the Peltier devices. The value of current flowing through the Peltier devices is not constant but is approximately 1.9–2.3 A, since it varies with the temperature of the devices' surface and other factors.

The motor is stopped when the temperature of the motor surface (bottom surface) reaches 100°C or when the temperature has hardly risen for a certain period of time.

4. Experimental Results and Discussion

4.1. Result

Figure 7 shows the measured temperatures for the thermoelectric cooling module (A), water cooling (B) and the motor alone (C) patterns when the motor is driven at 3.14 A. In the case of the thermoelectric cooling module, the temperature initially decreased, then increased and then remained almost constant at about 34°C above the temperature at 0 seconds. When water cooling was used, the temperature did not change much after a rise of about 43.5°C. On the other hand, in the case of the motor alone, the temperature continued to rise and reached 100°C after about 600 seconds. The measured temperature when the motor alone is driven at 1.57 A (C′) is shown in Figure 8. Temperature changes are also shown in Table 1 for each specific time.

The value of the voltage applied to the motor in each pattern when the motor is driven at 3.14 A (A, B and C) is shown in Figure 9. In the case of the thermoelectric cooling module and water cooling, the voltage value continued to increase at the beginning, but the increase became smaller and remained constant at around 15.5 V and 16.4 V,
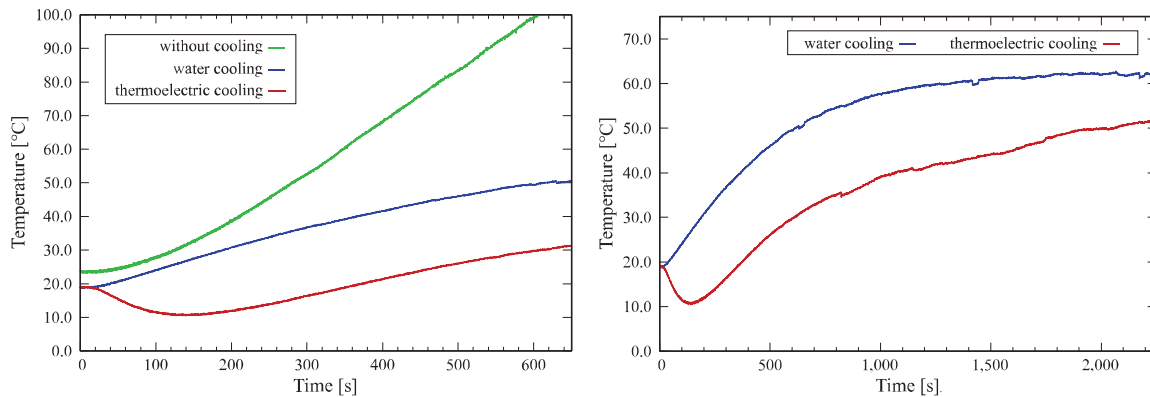

Fig. 7. Temperature at the bottom of the motor in the three patterns when the motor is driven at a constant current of 3.14 A.
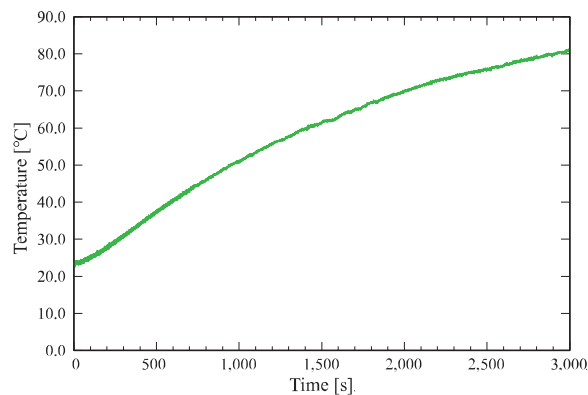

Fig. 8. Temperature at the bottom of the motor when driven at a constant current of 1.57 A when the DC motor is used alone.

Table 1. Variation of temperature in each condition

Time [seconds]	A [°C]	B [°C]	C [°C]	C′ [°C]
0	19.0	18.9	23.6	23.8
30	-1.3	+0.8	+0.2	+0.0
60	-4.6	+2.6	+1.5	+0.5
120	-8.1	+6.7	+6.0	+1.7
200	-7.0	+12.0	+15.2	+4.0
400	+2.6	+23.0	+44.8	+10.3
600	+10.8	+30.8	+75.8	+16.7
800	+16.0	+36.0	/	+22.3
1,000	+20.2	+39.1	/	+27.4
1,200	+22.2	+40.9	/	+32.0
1,400	+24.2	+41.8	/	+36.1
1,600	+26.1	+42.6	/	+39.2
1,800	+29.4	+43.5	/	+43.1
2,000	+30.9	+43.4	/	+46.0
2,200	+32.5	+43.5	/	+49.1
2,400	+33.1	/	/	+51.2
2,600	+33.7	/	/	+53.1
2,800	+33.5	/	/	+55.2
3,000	+33.9	/	/	+57.2

Note: Motor is driven at 3.14 A, using thermoelectric cooling module (A), water cooling (B) and no cooling (C). The motor alone is driven at 1.57 A (C′).
'/' indicates the time after the motor drive is stopped.
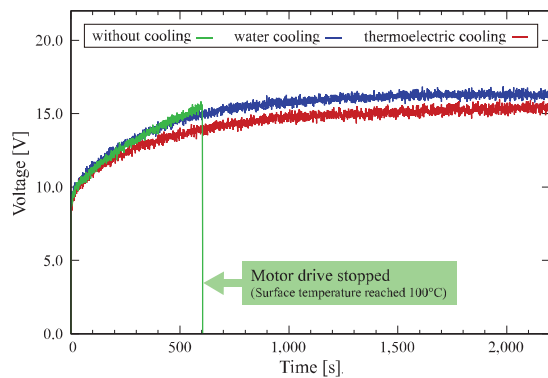
Fig. 9. Voltage values when the motor is driven at 3.14 A for the three patterns.

respectively. On the other hand, in the case of the motor alone, the upward trend remained at approximately 600 seconds, when the motor surface reached 100°C and the drive was stopped. The measured voltage when the motor alone is driven at 1.57 A (C′) is shown in Figure 10.

4.2. Discussion

For the case where the motor is driven at 3.14 A, it can be seen that the rise in surface temperature of the motor is significantly reduced when a thermoelectric cooling module is used and when water cooling is used, compared to the case where motor alone is used. The surface temperature is always lower when the motor is driven at 3.14 A with the thermoelectric cooling module than when the motor alone is driven at 1.57 A.
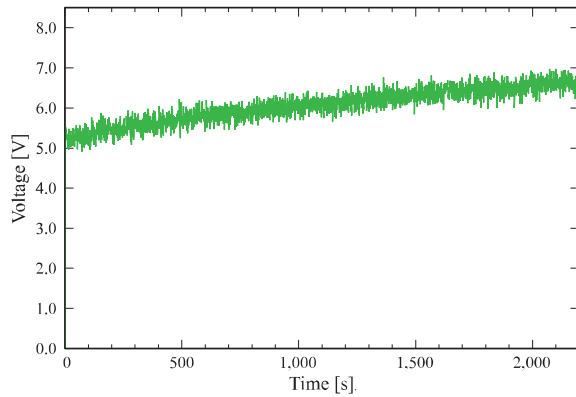
Fig. 10. Voltage value when the motor is driven at 1.57 A in the case of a DC motor alone.

Table 2. Approximate ratio of voltage and current applied to the motor (voltage value/current value)

Time [seconds]	A [V/A]	B [V/A]	C [V/A]	C' [V/A]
100	3.55	3.65	3.55	3.40
200	3.85	4.00	3.95	3.45
300	4.10	4.25	4.20	3.55
400	4.20	4.50	4.50	3.60
500	4.30	4.65	4.70	3.70
600	4.45	4.80	4.95	3.70
700	4.50	4.90	/	3.75
800	4.60	4.95	/	3.75
900	4.65	5.00	/	3.85
1,000	4.70	5.05	/	3.85
1,200	4.75	5.10	/	4.90
1,400	4.80	5.15	/	4.00
1,600	4.80	5.20	/	4.10
1,800	4.90	5.20	/	4.15
2,000	4.90	5.20	/	4.20
2,200	4.95	5.20	/	4.20
2,400	4.95	/	/	4.30
2,600	4.95	/	/	4.30
2,800	4.95	/	/	4.35
3,000	4.95	/	/	4.35
3,200	4.95	/	/	4.40

Note: Motor is driven at 3.14 A, using thermoelectric cooling module (A), water cooling (B) and no cooling (C). The motor alone is driven at 1.57 A (C'). '/' indicates the time after the motor drive is stopped.

In the case of water cooling, the temperature increase stopped when the temperature rose about 43.5°C from the start of motor drive, whereas in the case of thermoelectric cooling, the rise in temperature was about 34°C. It can be seen that the thermoelectric cooling module reduces the rise in motor temperature compared to water cooling.

Consider the voltage value of a DC motor when driven at a constant current. The voltage applied to the DC motor to drive the same magnitude of current was smaller with the thermoelectric cooling module than with the others. This is because the cooling with the thermoelectric cooling module suppressed the rise in temperature of the motor core and thus the coil resistance was relatively small. Since the back-electromotive force also affects the voltage value, it is difficult to directly calculate the resistance value of the motor being driven. However, since

the motor was not rotating at high speed and no significant difference in rotation speed was observed, the value obtained by dividing the voltage by the current can be used as an indicator.

The resistance of the motor's coils R_e, in relation to the temperature of the motor core T_C, is expressed by the following equation:

$$R_e = K_1 T_C + K_0. \tag{1}$$

The internal temperature can be inferred from the resistance of the coil because it increases linearly with rise in temperature. Therefore, the voltage applied to the motor divided by the current is a reference for the internal temperature.

The values of the voltage applied to the motor divided by the current are shown in Table 2. When the motor alone was driven at 3.14 A, the value at around 600 seconds, the timing at which the surface temperature reached 100°C, was 4.95 V/A. This value is almost the same as the value for the time period when the thermoelectric cooling module was used and the voltage stopped increasing. In the case of water cooling, it reached 4.95 V/A at around 800 seconds, then continued to rise and stopped rising from 5.20 V/A after 1,600 seconds. In the case of the motor alone, the voltage values continued to rise and would have been much larger if the motor continued to be driven.

When the thermoelectric cooling module was used, no rise above 4.95 V/A was observed, indicating that the internal temperature was kept to a certain degree lower than with water cooling. After 3,000 seconds, the value was still lower than the value at 900 seconds for the case of water cooling. Noting the value of 4.95 V/A, it can be inferred that the temperature of the motor core during thermoelectric cooling is close to the value after 600 seconds for the motor alone or 800 seconds for water cooling, even after a long drive time. It can be seen that cooling by the thermoelectric effect is also effective in cooling the inside of the motor.

Comparing the temperature of the motor surface with the change in the value of the ratio of voltage to current also confirms that there is a large time lag before the cooling of the surface affects the internal temperature. In particular, as can be seen from Figure 9, for water cooling and the motor alone, there was little difference in the change in voltage values in the first 300 seconds or so. It can be seen that the thermoelectric cooling module is effective in controlling the rise in internal temperature more quickly than water cooling, because heat is actively transferred compared to water cooling due to heat absorption by the Peltier devices.

On the other hand, when the motor is driven at 3.14 A using the thermoelectric cooling module, the motor core temperature is expected to be higher than when the motor is driven at 1.57 A, although the increase in surface temperature is kept small.

In this experiment, continuous operation was performed at twice the value of the intermittent rating, but the effect of the large heat transfer by the Peltier devices would be greater if intermittent operation was performed. In addition, although a DC motor was used in this case, it is thought that the effect of cooling would be greater if a type of motor in which the coil resides on the outside were used. Since even DC motors with high thermal resistance and poor cooling performance showed certain benefits relative to the use of the thermoelectric cooling module, it can be expected that the use of the thermoelectric cooling module can increase the upper limit of the current value that can continue to be driven for various types of motors.

In addition, when considered from the aspect of power consumption, the Peltier devices consume a lot of power, making them much less efficient than water cooling. This can be a major drawback of thermoelectric cooling modules, especially when used in industry. The principle of thermoelectric cooling in Peltier devices is a reversible reaction, and energy regeneration by thermoelectric power generation using the temperature difference due to motor heating can be considered. As a future issue, we believe it is necessary to attempt to reduce power consumption.

5. Conclusions

In this study, the thermoelectric cooling module was used to cool a motor driven continuously for a long period of time at a constant current twice the intermittent rating, and its performance was compared with the case of motor alone or water cooling. The surface temperature of the motor by itself reached 100°C in approximately 10 minutes, but even after 50 minutes of continuous driving, the temperature was kept below 55°C, significantly reducing the rise in temperature.

The internal temperature is more important than the surface temperature. From the voltage measurements, it was expected that the thermoelectric cooling module also suppresses the rise in internal temperature from an earlier stage compared to water cooling. Even after long periods of operation, the voltage remained nearly constant at lower voltages compared to water cooling, suggesting that the rise in internal temperature was maintained at a lower level than in other cases.

These experimental results show that the thermoelectric cooling module can be used to increase the upper limit of current at which the motor is continuously driven. It is shown that adding thermoelectric cooling to water cooling can provide more effective motor cooling for high-power motor drives.

Acknowledgements

References

Alencar Almeida, C. H., Da Rocha Souto, C., Veronese, J. P. and Carlos de Oliveira Custódio, J. (2015). Characterization of thermoelectric cell for electric power generation. In: *IEEE International Instrumentation and Measurement Technology Conference (I2MTC) Proceedings*, Pisa, Italy, 2015, pp. 1358–1362.

Belovski, I., Ivanov, K., Aleksandrov, A. and Aleksandrova, I. (2021). Regression Model of a Thermoelectric Generator based on Peltier Modules. In: *17th Conference on Electrical Machines, Drives and Power Systems (ELMA)*, Sofia, Bulgaria, 2021, pp. 1–5, 2021.

Guizzo, E. (2019). By leaps and bounds: An exclusive look at how Boston dynamics is redefining robot agility. *IEEE Spectrum*, 56(12), pp.34–39.

Gwoździewicz, M. and Zawilak, J. (2016). Single-Phase Line Start Permanent Magnet Synchronous Motor with Skewed Stator. *Power Electronics and Drives*, 1(2), pp. 187–194.

Katsura, S., Irie, K. and Ohishi, K. (2008). Wideband Force Control by Position-Acceleration Integrated Disturbance Observer. *IEEE Transactions on Industrial Electronics*, 55(4), pp. 1699–1706.

Katsura, S., Matsumoto, Y. and Ohnishi, K. (2003). Modeling of force sensing and validation of disturbance observer for force control. *IEEE Transactions on Industrial Electronics*, 54(1), pp. 530–538.

Kawaharazuka, K., Hiraoka, N., Tsuzuki, K., Onitsuka, M., Asano, Y., Okada, K., Kawasaki, K. and Inaba, M. (2020). Estimation and Control of Motor Core Temperature With Online Learning of Thermal Model Parameters: Application to Musculoskeletal Humanoids. *IEEE Robotics and Automation Letters*, 5(3), pp.4273–4280.

Kim, D., Ahn, J., Campbell, O., Paine, N. and Sentis, L. (2018). Investigations of a Robotic Test Bed With Viscoelastic Liquid Cooled Actuators. *IEEE/ASME Transactions on Mechatronics*, 23(6), pp. 2704–2714.

Kumagai, I., Noda, S., Nozawa, S., Kakiuchi, Y., Okada, K. and Inaba, M. (2014). Whole body joint load reduction control for high-load tasks of humanoid robot through adapting joint torque limitation based on online joint temperature estimation. In: *IEEE-RAS International Conference on Humanoid Robots*, Madrid, Spain, 2014, pp. 463–468.

Kumar, B. V. R. and Kumar, K. S. (2016). Design of a new Dual Rotor Radial Flux BLDC motor with Halbach array magnets for an electric vehicle. In: *IEEE International Conference on Power Electronics, Drives and Energy Systems (PEDES)*, Trivandrum, India, 2016, pp. 1–5.

Liu, K., Yin, M., Hua, W., Ma, Z., Lin, M. and Kong, Y. (2018). Design and Analysis of Halbach Ironless Flywheel BLDC Motor/Generators. *IEEE Transactions on Magnetics*, 54(11), pp.1–5.

Nizam, M., Waloyo, H. T., Mujianto, A., Inayati and Purwanto, A. (2014). Brushless DC motor torque improvement with mgnetic material stator core. In: *International Conference on Electrical Engineering and Computer Science (ICEECS)*, Kuta, Bali, Indonesia, 2014, pp. 158–162.

Pourkiaei, S. M., Ahmadi, M. H., Sadeghzadeh, M., Moosavi, S., Pourfayaz, F., Chen, L., Pour Yazdi, M. A. and Kumar, R. (2019). Thermoelectric cooler

and thermoelectric generator devices: A review of present and potential applications, modeling and materials. *Energy*, 186, pp. 1–17.

Quintal-Palomo, R., Dybkowski, M. and Gwoździewicz, M. (2016). Parametric Analysis for the Design of a 4 Pole Radial Permanent Magnet Generator for Small Wind Turbines. *Power Electronics and Drives*, 1(2), pp. 175–186.

Ramesh, P. and Lenin, N. C. (2019). High Power Density Electrical Machines for Electric Vehicles—Comprehensive Review Based on Material Technology. *IEEE Transactions on Magnetics*, 55(11), pp.1–21.

Sarac, V. and Stefanov, G. (2020). Various Rotor Topologies of Line-Start Synchronous Motor for Efficiency Improvement. *Power Electronics and Drives*, 5(1), pp. 83–95.

Seok, S., Wang, A., Chuah, M. Y., Hyun, D. J., Lee, J., Otten, D. M., Lang, J. H. and Kim, S. (2015). Design Principles for Energy-Efficient Legged Locomotion and Implementation on the MIT Cheetah Robot.

IEEE/ASME Transactions on Mechatronics, 20(3), pp. 1117–1129.

Sevinchan, E., Dincer, I. and Lang, H. (2018). A review on thermal management methods for robots. *Applied Thermal Engineering*, 140, pp.799–813.

Siyang, L., Lam, K. H. and Cheng, K. W. E. (2016). Development of a motor waste heat power generation system based on thermoelectric generators. In: *International Symposium on Electrical Engineering (ISEE)*, Hong Kong, China, 2016, pp. 1–5.

Toren, M. and Mollahasanoglu, H. (2021). Investigation of Thermoelectric Cooler System Effect on Induction Motor Performance. In: *17th Conference on Electrical Machines, Drives and Power Systems (ELMA)*, Sofia, Bulgaria, 2021, pp. 1–4.

Urata, J., Nakanishi, Y., Okada, K. and Inaba, M. (2010). Design of high torque and high speed leg module for high power humanoid. In: *IEEE/RSJ International Conference on Intelligent Robots and Systems*, Taipei, Taiwan, 2010, pp. 4497– 4502.